Supporting Information

Wang et al. 10.1073/pnas.1405411111

SI Methods

Generation of *Shox2*^{HA} Allele. To generate the *Shox2*^{HA} allele, we used an 8.3-kb *Flag-HA-Shox2a-DsRed-polyA* sequence with an Frt flanking neomycin-resistance cassette driven by the PGK promoter (PGK-neo), which contains the mouse *Shox2* gene cDNA as indicated in Fig. 4*H*. To replace the endogenous DNA sequence (the 5′ arm covers almost half of exon1 and intron1 whereas the 3′ arm covers almost half of Exon2) with the *Flag-HA-Shox2a-DsRed-polyA* sequence, we constructed a targeting vector containing a 5.6-kb homologous arm upstream of the translational starting codon (ATG) of the *Flag-HA-Shox2a-DsRed-polyA* sequence and a 2.9-kb homologous arm downstream of the PGK-neo cassette. A diphtheria toxin expression cassette (DTA) was placed upstream of the 5′ homology arm to prevent random insertion. The targeting vector was then linearized and introduced into G4 ES cells (1) by electroporation. ES clones grown under G418 selection were subsequently screened by long-range PCR followed by sequencing of PCR products. PCR amplification on DNA samples from genuinely targeted clones by forward primer on 5′ flanking region out of the 5′ homology arm (5′ Forward) and reverse primer on DsRed (DsRed reverse) yielded a 7.2-kb band; PCR by forward primer on the neomycin-resistance cassette (Neo-forward) and reverse primer out of the 3′ homology arm on the 3′ flanking region yielded a 3.6-kb band. The correctly targeted clone was injected into blastocysts to create chimera mice. Chimeras were crossed with CD-1 females (Charles River) to generate F1 mice and subsequently were genotyped by long-range PCR. The oligo sequences were as follows: 5′ forward oligo sequence, 5′-AGTTTGGGAGATGAGGGAAAACCATCATCAGAATATATTGTATACAG-3′; DsRed reverse oligo sequence, 5′-ACACCTTGGAGGCGTACTGG-3′; Neo-forward oligo sequence, 5′-CGAAACGATCCTCATCCTGT-3′; and 3′ reverse oligo sequence, 5′-GGACCAGCCTCTGTATTGGA-3′.

Microarray for miRs. Total RNA from embryonic day 13.5 (E13.5) mouse embryonic hearts was extracted and purified using the mirVana microRNA (miR) Isolation Kit (Ambion). RNA samples were labeled and analyzed by LC Sciences using an mParaflo Microfluidic Biochip technology as previously described (2).

Chromatin Immunoprecipitation and Real-Time PCR Validation. E13.5 hearts were collected from the paired-like homeodomain transcription factor 2 (*Pitx2*)^{Flag} allele and followed by ChIP analysis as previously described (3). The Pitx2 binding regions were validated using real-time PCR. The real-time PCR primers for amplifying the Pitx2 regulatory element in *mir-17-92* and *mir-106b-25* genomic sequence were as follows: sense, 5′-CTCAGGTACTGGTCGCGAAG-3′, antisense, 5′-GGGAGACGAGTCACATCCAC-3′ (for *mir-17-92* region1, 159 bp); sense, 5′-TGGTTCTTAGGTGACCAGAGGGAA-3′, antisense, 5′-AGCAGCAAGCCTGAACTCTACTGT-3′ (for *mir-17-92* region2, 186 bp); sense, 5′-ACCTGGTATGACTTCAGGTTTATT-3′, antisense, 5′-ATGGTAAGAACAGTCCAAGGATAG-3′ (negative control for *mir-17-92*, 226 bp); sense, 5′-AAACACTAAGGCCTCTGGAAG-3′, antisense, 5′-CGCCCTCTAAAGTCAGTTCTC-3′ (for *mir-106b-25* region1, 165 bp); sense, 5′-GACTAGCCAGGTGGAAAGATAG-3′, antisense, 5′-TCCAGAACCGCCATGATTT-3′ (for *mir-106b-25* region 2, 172 bp); and sense, 5′-CTCTGGTCTTCCCGAATGTTAG-3′, antisense, 5′-GGCGAAATATCGAAGTGATGAAC-3′ (negative control for *mir-106b-25*, 241 bp).

ChIP-Sequencing and ChIP-Seq Analysis. ChIP was performed using 3-mo-old hearts from the *Pitx2*^{Flag} allele. DNA libraries were generated according to the manufacturer's instruction (4471252; Life Technologies), and sequencing was performed on an Ion Torrent PGM system. Fragments of the completed DNA library ranged from ∼170–220 bp in length. For ChIP-Sequencing (ChIP-Seq) analysis, Ion torrent PGM reads were aligned to the mm9 (National Center for Biotechnology Information Build 37) assembly using Torrent Suite (2.0.1) Ion-alignment (2.0.3–1). The ChIP-Seq signal was normalized to a total of 10 million reads and visualized in the University of California Santa Cruz genome browser. ChIP enriched peaks were identified using Homer (4) by the default setting, as read number enriched at least fourfold over background signal and Poisson *P* value less than 1.00e−4 were required. Nearest genes associated to the enriched peaks were annotated using Homer annotate Peaks function.

X-Gal Staining. All embryos were dissected in PBS and stained with X-gal using a whole-mount β-galactosidase staining protocol as previously described (5).

Quantification of the Atrial Weight. To determine whether *Nkx2.5*^{Cre}*; mir-17-92*$^{flox/flox}$*; mir-106b-25*$^{null/+}$ mutants have structural remodeling atrium, hearts were collected from both 10-wk-old mutants and control mice. A total of four *Nkx2.5*^{Cre}*; mir-17-92*$^{flox/flox}$*; mir-106b-25*$^{null/+}$ mutants and six controls (*Nkx2.5*^{Cre} $n = 3$, and *mir-17-92*$^{flox/flox}$*; mir-106b-25*$^{null/+}$ $n = 3$) were compared. Heart pictures were taken, and there was no obvious morphological difference. The atrium of each mouse was weighted and normalized to its body weight for comparison.

Cardiac Electrophysiology. In vivo electrophysiology in mice was conducted as previously described (6). Surface and intracardiac electrophysiology parameters were assessed at baseline. Right atrial pacing was performed using 2-ms current pulses delivered by an external stimulator (STG-3008, Multi Channel Systems). Sinus node recovery time (SNRT), which is defined as the interval between the last stimulus of the pacing train and onset of the first spontaneous sinus beat, was measured after applying a 15-s atrial-pacing train at a basic cycle length of 100 ms (6). Atrial effective refractory period (AERP) and the effective refractory period of the atrioventricular effective refractory period (AVERP) were determined by applying a series of atrial-pacing trains at a fixed basic cycle length of 100 ms (S1) with an S2 premature stimulus. The S1–S2 interval was progressively reduced by 2 ms in each pacing train from 70 ms to 20 ms (6). The AERP is defined as the longest S1–S2 coupling interval for atria that failed to generate a propagated beat with S2 (6). The AVERP is defined as the longest S1–S2 coupling interval at which the premature stimulation delivered to the atrium is followed by a His potential but not by a QRS (the duration of the interval between the beginning of the Q wave to the peak of the S wave) complex (6).

Immunofluorescence. Embryos were fixed in 10% neutral buffered formalin, embedded in paraffin, cut into 5-μm sections, and then mounted on Superfrost/Plus slides. The antigens were retrieved by 2-min incubation in the 10-mM citrate buffer in a microwave oven. The primary antibody Shox2 (generated in the Y.C. laboratory) was used at 1:200 dilution. Broad HRP-conjugated secondary antibody (Invitrogen) was used and visualized using TSA Plus Fluorescence Systems from PerkinElmer on a Zeiss

LSM 510 Confocal Microscope. Nuclei were stained with 4,6-diamidino-2-phenylindole (DAPI).

RT-PCR and Real-Time PCR. Total RNA was isolated from embryonic hearts using an RNeasy Micro Kit (QIAGEN), followed by RT-PCR using Super Script II reverse transcriptase (Invitrogen). Real-time thermal cycling was performed using StepOne Real-Time PCR Systems (Applied Biosystems) with SYBR Green JumpStart *Taq* ReadyMix (Sigma).

Whole-Mount in Situ Hybridization. Whole-mount in situ hybridization was performed as previously described (5). The gene probes were synthesized using a DIG RNA Labeling Kit (Roche) following the manufacturer's guidelines. The enzymes used for digestion and transcription of in situ constructs were XhoI and T7 for *Shox2* (from the Y.C. laboratory) and PstI and T3 for *Tbx3* (gifts from the Robert Kelly laboratory, Institut de Biologie du Développement de Marseille, Marseille Cedex, France). For all experiments, at least three mutants and control embryos were analyzed for each probe.

Generation of Constructs and Site-Directed Mutagenesis. Detailed information about generation of these constructs and site-directed mutagenesis was previously described in ref. 7. Briefly, to generate 3′ UTR Luciferase reporter plasmids, 3′ UTR genomic sequences of *Shox2* and *Tbx3* were amplified, using a high-fidelity PCR system (Roche) with designed oligonucleotides, and subcloned into the pMIR-REPORT Luciferase miR Expression Reporter Vector (Ambion). All PCR products were sequenced to confirm sequence integrity. Site-directed mutagenesis was achieved by using the QuikChange II site-directed mutagenesis kit (Agilent).

Luciferase Activity Assay. P19 cells (ATCC) were transfected using Lipofectamine 2000 (Invitrogen). miR mimics used for transfection were purchased from Thermo Scientific. Reporter plasmids used for transfection were described in *Generation of Constructs and Site-Directed Mutagenesis*. Luciferase activity assays were measured using the Luciferase Assay System (Promega).

1. George SH, et al. (2007) Developmental and adult phenotyping directly from mutant embryonic stem cells. *Proc Natl Acad Sci USA* 104(11):4455–4460.
2. Wang J, et al. (2010) Bmp signaling regulates myocardial differentiation from cardiac progenitors through a MicroRNA-mediated mechanism. *Dev Cell* 19(6):903–912.
3. Wang J, et al. (2010) Pitx2 prevents susceptibility to atrial arrhythmias by inhibiting left-sided pacemaker specification. *Proc Natl Acad Sci USA* 107(21):9753–9758.
4. Heinz S, et al. (2010) Simple combinations of lineage-determining transcription factors prime cis-regulatory elements required for macrophage and B cell identities. *Mol Cell* 38(4):576–589.
5. Lu MF, Pressman C, Dyer R, Johnson RL, Martin JF (1999) Function of Rieger syndrome gene in left-right asymmetry and craniofacial development. *Nature* 401(6750): 276–278.
6. Li N, et al. (2012) Inhibition of CaMKII phosphorylation of RyR2 prevents induction of atrial fibrillation in FKBP12.6 knockout mice. *Circ Res* 110(3):465–470.
7. Wang J, et al. (2013) MicroRNA-17-92, a direct Ap-2α transcriptional target, modulates T-box factor activity in orofacial clefting. *PLoS Genet* 9(9):e1003785.

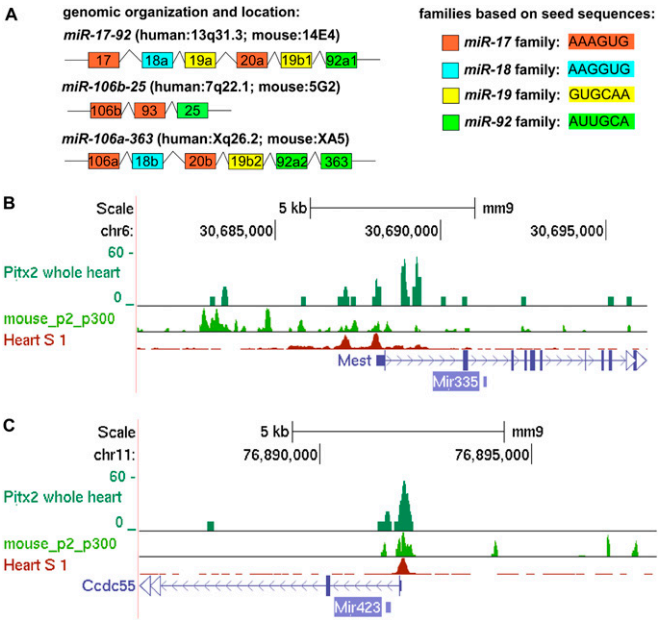

Fig. S1. (*A*) The genomic structure and location of *miR-17-92* and its two orthologous clusters *miR-106b-25* and *miR-106a-363* are shown *Left*. Three miR clusters are grouped into different families based on their seed sequence (shown *Right*). miRs with the same seed sequence are indicated in the same color. (*B* and *C*) Three-month-old mouse whole-heart ChIP-Seq enrichment profiles (GSE50401) (1) for Pitx2 bound loci upstream of *mir-335* and *mir-423*. The peaks from different datasets including Pitx2 ChIP-Seq (GSE50401) (1), P2 heart p300 ChIP-Seq (GSE32587) (2), and 8-wk-old heart DNase I Hypersensitive Site Seq (ENCODE) are aligned for comparison.

1. Tao Y, et al. (2014) Pitx2, an atrial fibrillation predisposition gene, directly regulates ion transport and intercalated disc genes. *Circ Cardiovasc Genet* 7(1):23–32.
2. May D, et al. (2011) Large-scale discovery of enhancers from human heart tissue. *Nat Genet* 44(1):89–93.

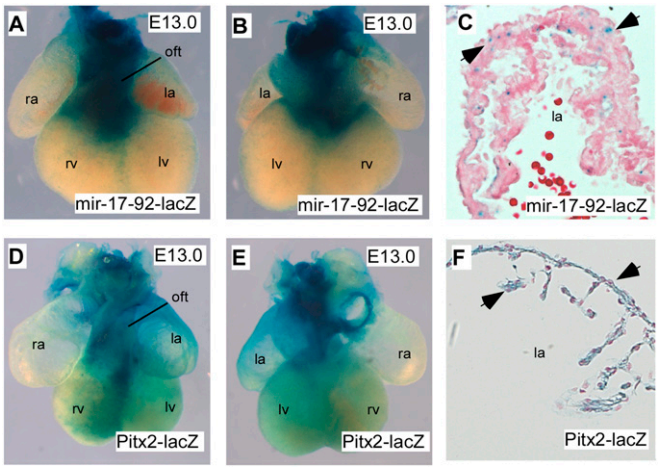

Fig. S2. *mir-17-92* expression overlaps with *Pitx2* expression. (*A* and *B*) β-Gal–stained embryonic heart of *mir-17-92-lacZ* BAC transgenic mice at E13.0. (*C*) Sectioning of LacZ-stained E13.0 embryonic heart indicated *mir-17-92* expression in myocardium of left atrium. (*D* and *E*) β-Gal–stained embryonic heart of *Pitx2-lacZ* allele mice at E13.0. (*F*) Sectioning of LacZ-stained E13.0 embryonic heart indicated *Pitx2* expression in myocardium of left atrium. Arrows designate lacZ activities. la, left atrium; lv, left ventricle; oft, out flow tract; ra, right atrium; rv, right ventricle.

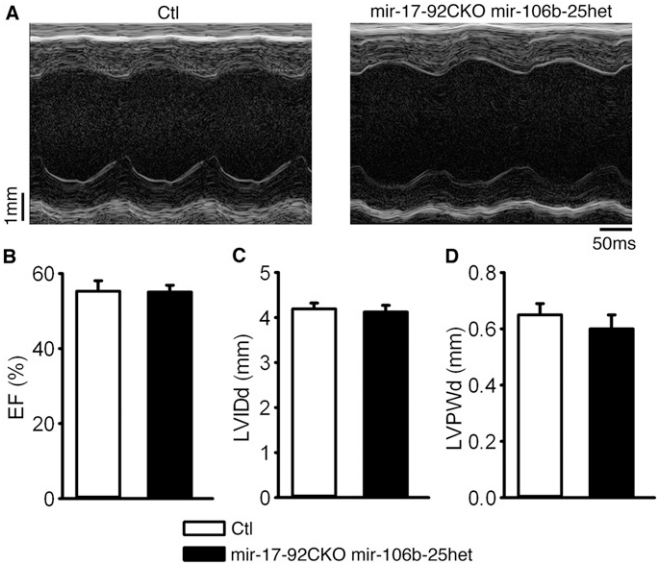

Fig. S3. *mir-17-92* CKO *mir-106b-25* het mice preserved normal cardiac contractility and dimensions at the age of 4 mo. (*A*) Representative M-mode echocardiogram traces in control (Ctl) and *mir-17-92* CKO; *mir-106b-25* het mice at the age of 4 mo. (*B*) Ejection fraction (%). (*C*) Diastolic left-ventricular internal dimension ($LVID_d$). (*D*) Diastolic left-ventricular posterior-wall thickness ($LVPW_d$). Data were collected from seven Ctl mice and six *mir-17-92* CKO; *mir-106b-25* het mice.

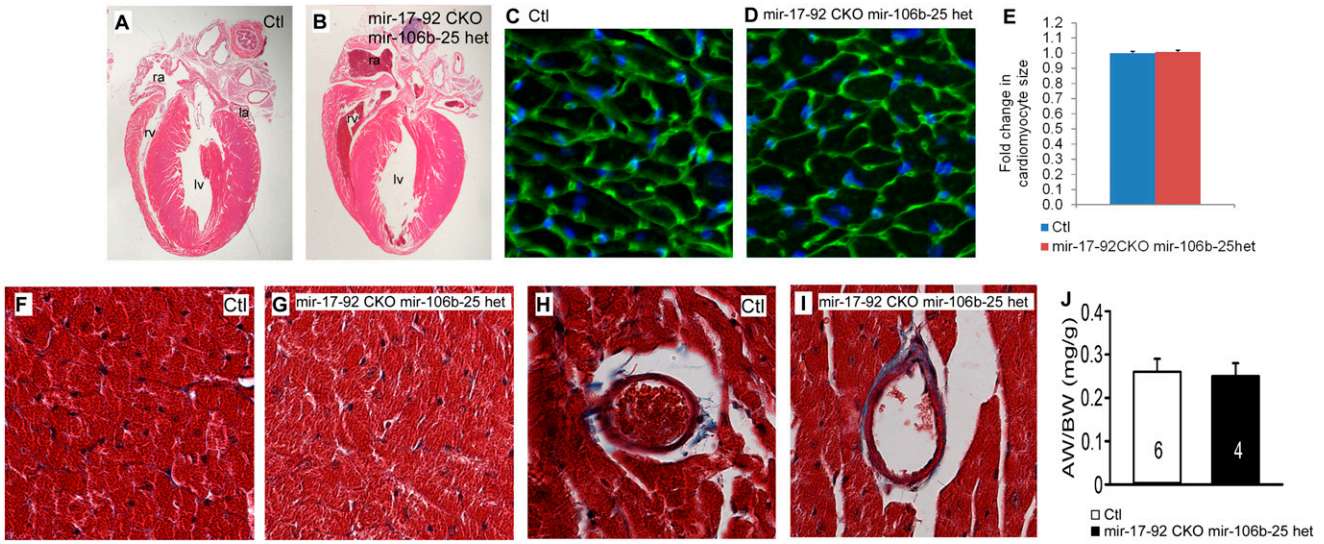

Fig. S4. mir-compound mutant mice did not have obvious abnormal cardiac structure and change of fibrosis level. (*A* and *B*) Hematoxylin/eosin (H&E) staining in *Nkx2.5*^{Cre}*; mir-17-92*$^{flox/flox}$*;mir-106b-25*$^{null/+}$ mutants ($n = 10$) and their littermate *mir-17-92*$^{flox/flox}$*; mir-106b-25*$^{null/+}$ control mice ($n = 4$) at the age of 4 mo. Compared with control (*A*), *Mir-17-92* CKO; *mir-106b-25* het mice (*B*) didn't show histological change in ventricular morphology at 4 mo of age. (*C–E*) Wheat germ agglutinin (WGA) staining in *Nkx2.5*^{Cre}*; mir-17-92*$^{flox/flox}$*; mir-106b-25*$^{null/+}$ mutants ($n = 3$) and *mir-17-92*$^{flox/flox}$*; mir-106b-25*$^{null/+}$ controls ($n = 3$) at 4 mo old. Cardiomyocyte cell size of ventricular myocardium has no significant change in mutants compared with controls. Mean ± SEM, $^*P > 0.05$. (*F–I*) Masson's Trichrome staining in *Nkx2.5*^{Cre}*; mir-17-92*$^{flox/flox}$*; mir-106b-25*$^{null/+}$ mutants (*F* and *H*, $n = 3$) and controls (*G* and *I*, $n = 3$) revealed no significant difference in mutants compared with controls. (*J*) Bar graph summarizing the ratio of atrial weight to body weight (AW/BW) in each group at 10 wk. Numbers inside bars indicate the number of mice studied. *Nkx2.5*^{Cre}*; mir-17-92*$^{flox/flox}$*; mir-106b-25*$^{null/+}$ mutants ($n = 4$) and controls (*Nkx2.5*^{Cre} $n = 3$, and *mir-17-92*$^{flox/flox}$*; mir-106b-25*$^{null/+}$ $n = 3$) revealed no significant difference in mutants compared with controls. Mean ± SEM, $^*P > 0.05$. AW, atrial weight; BW, body weight.

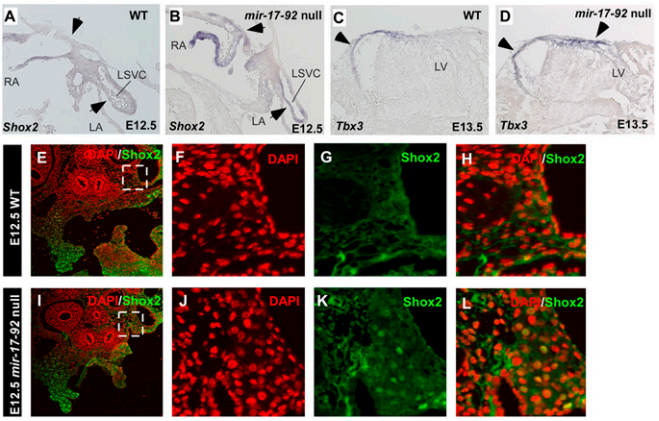

Fig. S5. *miR-17-92* and *miR-106b-25* represses *Shox2* and *Tbx3*. (*A–D*) *miR-17-92* represses *Shox2* and *Tbx3* in vivo. Transverse sections through inflow of heart after whole-mount in situ hybridization with indicated probes in E12.5 and E13.5 control and mutant embryos. Genotypes and probes are labeled. Arrows designate gene expression. LA, left atrium; LV, left ventricle; LSVC, left superior vena cava; RA, right atrium. (*E–L*) Immunofluorescence shows expression of Shox2 is higher in E12.5 left superior caval vein of *miR-17-92* null embryos (*I–L*) compared with wild type embryos (*E–H*). Boxed areas in *E* and *I* are correspondingly shown at higher magnification in *F–H* and *J–L*. Nuclei (red)-stained with DAPI. White arrows designate Shox2-expressing cells.

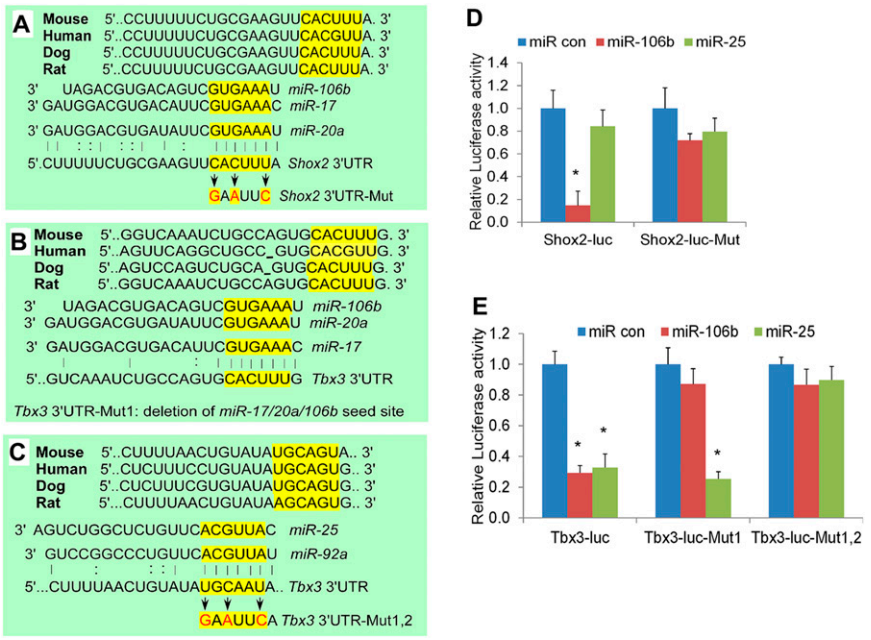

Fig. S6. *miR-17-92* and *miR-106b-25* directly represses *Shox2* and *Tbx3*. (*A–C*) Phylogenetic sequence alignment of *miR-17-92/mir-106b-25* family seed sequence in 3′ UTR of *Shox2* and *tbx3*. Respective *mir-17-92/mir-106b-25* family seed sequence in 3′ UTR of *Shox2* (*A*) and *Tbx3* (*B* and *C*) are highlighted in yellow, and mutated nucleotides are highlighted in red. (*D* and *E*) *miR-106b-25* directly represses *Shox2* and *Tbx3* in vitro. Luciferase reporter assays in P19 cell line with reporters and miRs as labeled. Mean ± SEM, $*P < 0.05$.

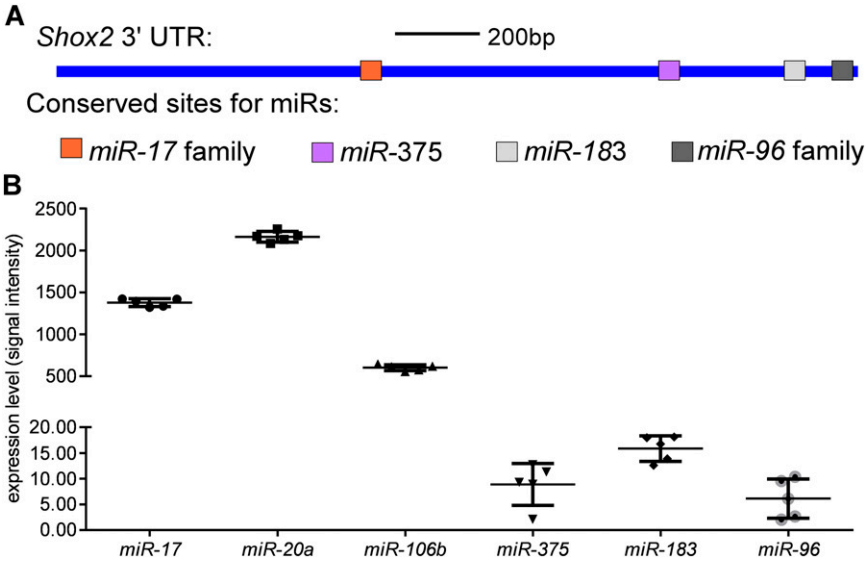

Fig. S7. (*A*) Locations of four conserved seed sites of different miRs/miR families in 3′ UTR of *Shox2* are as indicated. (*B*) miR profiling data indicated that *miR-17* family is expressed in the E13.5 wild-type embryonic heart whereas the other miRs/miR families are barely expressed.

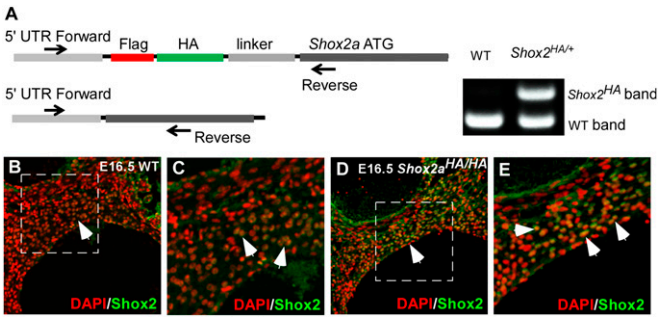

Fig. S8. (*A*) PCR strategy and gel picture for genotyping *Shox2a*$^{HA/Neo}$ allele. (*B–E*) Immunofluorescence shows that expression of Shox2 is higher in E16.5 sinoatrial node (SAN) of *Shox2a*$^{HA/HA}$embryos (*D* and *E*) compared with wild-type embryos (*B* and *C*). Boxed areas in *B* and *D* are correspondingly shown at higher magnification in *C* and *E*. Nuclei (red)-stained with DAPI. White arrows designate Shox2-expressing cells.

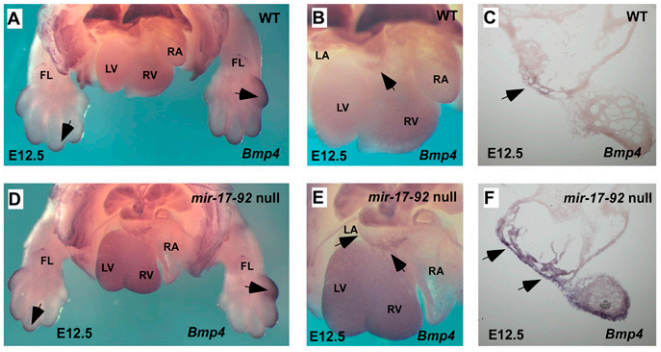

Fig. S9. Whole-mount in situ hybridization and sectioning indicated up-regulated expression of *Bmp4* in E12.5 left superior caval vein and coronary sinus of *miR-17-92*–null embryos (*D–F*) compared with wild-type embryos (*A–C*). Black arrows designate *Bmp4*-expressing cells. FL, fore limb; LA, left atrium; LV, left ventricle; OFT, out flow tract; RA, right atrium; RV, right ventricle.

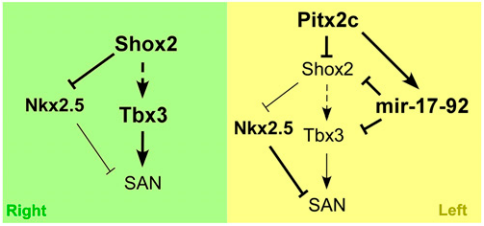

Fig. S10. Model for *Pitx2-miR* genetic pathway prevents susceptibility to atrial fibrillation. Sinoatrial node (SAN) program is active without Pitx2 expression on the right of heart. On the left of heart, Pitx2 directly inhibits the Shox2-directed pathway and activates the *miR-17-92*/*miR-106b-25*–mediated pathway to promote the formation of atrial working myocardium. The dashed arrow indicates a genetic relationship that may be indirect.

Table S1. Baseline cardiac electrophysiological parameters in different genotypes

Parameters	WT	miR-17-92 Het	miR106b-25 Het	miR106b-25 Homo
HR, bpm	567 ± 13	556 ± 27	541 ± 8	550 ± 21
PR, ms	35.8 ± 1.3	32.7 ± 1.6	38.3 ± 1.1	36.0 ± 1.4
QRS, ms	8.8 ± 0.3	9.3 ± 0.3	10.1 ± 0.3	9.8 ± 0.2
QTc, ms	24.4 ± 0.8	24.1 ± 1.2	24.4 ± 0.8	24.7 ± 1.1
SNRT, ms	114.5 ± 7.9	130.4 ± 11.2	143.7 ± 6.2	142.0 ± 11.4
AERP, ms	40.0 ± 1.2	38.4 ± 2.7	41.9 ± 1.7	38.8 ± 2.0
AVERP, ms	46.0 ± 1.3	47.0 ± 1.7	51.1 ± 1.6	48.8 ± 1.4

All values expressed are mean ± SEM. AERP, atrial effective refractory period; AVERP, atrioventricular nodal effective refractory period; HR, heart rate; PR, interval from beginning of P waves to the peak of R wave; QRS, duration of interval between beginning of Q wave to peak of S wave; QTc, duration of Q-T interval corrected for heart rate; SNRT, sinus node recovery time. No significant difference between groups.

Table S2. Echocardiographic parameters of mir-17-92CKO, mir-106b-25Het mice and their control littermates at the age of 4 mo

Parameters	Ctl ($n = 7$)	mir-17-92CKO mir-106b-25Het ($n = 6$)
HR, bpm	431 ± 14	405 ± 20
Age, mo	4.7 ± 0.6	4.9 ± 0.4
EF, %	55.3 ± 2.8	55.0 ± 1.8
FS, %	28.6 ± 1.8	28.3 ± 1.2
$LVID_d$, mm	4.19 ± 0.13	4.12 ± 0.15
$LVID_s$, mm	2.96 ± 0.14	2.88 ± 0.10
$LVPW_d$, mm	0.65 ± 0.04	0.60 ± 0.05
$LVPW_s$, mm	0.78 ± 0.05	0.76 ± 0.04

Data are expressed as mean ± SEM. BW, body weight; HR, heart rate; EF, ejection fraction; FS, left ventricular fractional shortening; LVID, left ventricular internal dimension; LVPW, left ventricular posterior wall thickness. Subscript letters represent during diastole (d) or systole (s).